ELSEVIER

Ecological Modelling 84 (1996) 215–232

ECOLOGICAL MODELLING

Shock load modelling in the anaerobic digestion process

Stefano Marsili-Libelli *, Simone Beni

Dept. of Systems and Computers, University of Florence, Via S. Marta, 3-50139 Florence, Italy

Received 19 April 1994; accepted 21 June 1994

Abstract

A simplified mathematical model for the behaviour of anaerobic digesters under shock loading conditions is derived with a special emphasis on bicarbonate alkalinity. This study was motivated by the development of a novel bicarbonate alkalinity measuring device providing on-line information of this variable, which is particularly well suited for the early detection of organic overloading. The model includes a set of dynamic equations and an extended ion balance to describe the effect of alkali, volatile fatty acids and carbon dioxide. After the structural description, the model is calibrated using specific shock experimental data and its implications are discussed in terms of a variety of shock conditions. Lastly, the feasibility of bicarbonate dosing control is assessed through proportional-integral-derivative (PID) controller design and model simulation.

Keywords: Anaerobic digestion; Bacteria; Parameter estimation

1. Introduction

Anaerobic digestion is a widely used process to dispose of a wide variety of biodegradable wastes with the additional benefit of producing energy in the form of biogas. The process is based on a complex chain of biochemical reactions through which the waste is first partially transformed into volatile fatty acids and then converted into methane and carbon dioxide. Given this inherent complexity, the process is quite vulnerable to abrupt operating changes which, if unchecked, may eventually lead to a total process failure. Thus much importance has been given to early failure detection, so that in the event of a shock a preemptive remedial action can be taken to bring the process back into its normal operation. Mathematical models can assist in the description of shock behaviour and in the design of safeguard control systems. Though several excellent anaerobic digestion models of sufficient generality are already available in the literature (Rozzi and Passino, 1985; Rozzi et al., 1985a; McCarthy and Mosey, 1990; Siegrist et al., 1992), the task of developing a new one was undertaken with the specific objective of describing the dynamics of bicarbonate alkalinity under organic shock load conditions and how this could be controlled by alkali dosing. The literature on this aspect is already well developed (Rozzi, 1984; Rozzi et al., 1985b; Van Breusegem et al., 1990), but so far the majority of bicarbonate dosing control systems used pH measurement, which is rather unreliable, but on-line bicarbonate alkalinity monitor-

* Corresponding author. E-mail: marsili@ingfi1.ing.unifi.it

SSDI 0304-3800(94)00125-2

ing was so far not possible. Conversely, this new model was motivated by the availability of a new real-time bicarbonate alkalinity (BA) monitor. This device was recently developed at the University of Glamorgan and is already described in the literature (Hawkes et al., 1992,1993). This shock-oriented model takes into account the dynamics of BA as a result of an extended electro-neutrality balance including volatile fatty acids (here mainly assumed to be acetic acid) and carbon dioxide in both phases. The end use of the model is the design and implementation of control strategies for bicarbonate dosing to minimize the adverse effects of organic load shocks on digester operation.

Before considering the simplified shock model, the main pathways of anaerobic digestion are shown in Fig. 1, where volatile fatty acids are split into acetic acid on one side and propionic and butyric acid on the other. The reason for this is that they undergo different transformations which affect the overall process behaviour. Although acetic acid is the end product of substrate conversion into volatile fatty acids (VFA), other intermediate VFAs are also formed. The most important of these are propionic and butyric acids. They are mediated by obligate hydrogen producers, which are inhibited by the hydrogen they produce and are dependent on its removal by methanogens. The presence of hydrogen in the outlet gas is related to an increase of these acids.

The process model considered in this paper has the special purpose of describing how the system responds to organic load shock. It is there-

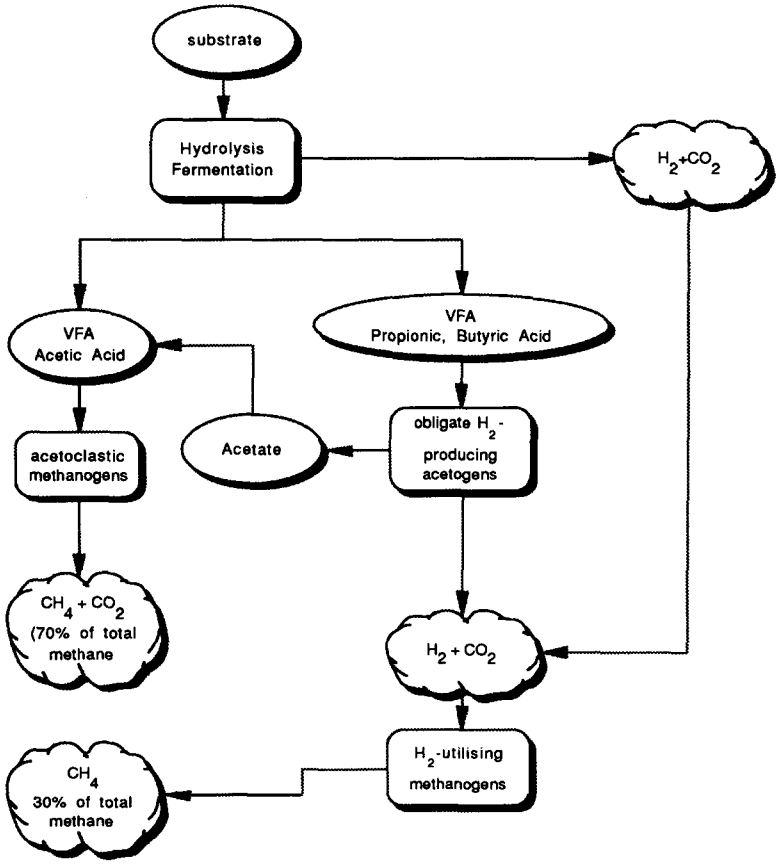

Fig. 1. Main pathways in the anaerobic digestion process.

fore deliberately simplified and is oriented towards modelling the behaviour of a normal digester in terms of bicarbonate alkalinity. For this reason, of all the volatile fatty acids only acetic acid is considered in the acidogenic stage. The hydrolytic fermentative and obligate H_2-producing acidogens are considered as one group of acidogens producing acetic acid. The resulting dynamics are described in Section 2. Other relevant process variables were included: bacterial populations (both acidogenic and methanogenic), substrate consumption, and carbon dioxide dynamics, both in the liquid and gas phase. To model bicarbonate alkalinity, an extended ion balance was developed which takes into account the interactions among all ion species, as illustrated in Section 3. Section 4 presents a steady-state analysis which reveals the difference between a stationary and a dynamic process operation. It shows in particular how the substantial transient behaviour that is observed during shock loading is primarily due to ion unbalance and is definitely a dynamic characteristic of the system. It is later shown that this additional steady-state model is instrumental for the subsequent computational scheme required for model calibration. The application of this technique and its results are discussed in Section 5. The data used for model calibration and validation were produced at the University of Glamorgan with the anaerobic filter pilot plant and the experimental conditions described in Hawkes et al. (1993). Section 6 discusses acidic acid shock, produced by model simulation, whereas Section 7 deals with bicarbonate dosing with a proportional-integral-derivative (PID) regulator.

2. Process model

The model is partly based on a previous paper by Marsili-Libelli and Nardini (1985) and also draws from a well established literature (Bailey and Ollis, 1986; Pavlostatis and Giraldo-Gomez, 1991) as far as bacterial kinetics are concerned. It is organized around the simplified interaction scheme of Fig. 2 showing the transfer coefficients between model stages.

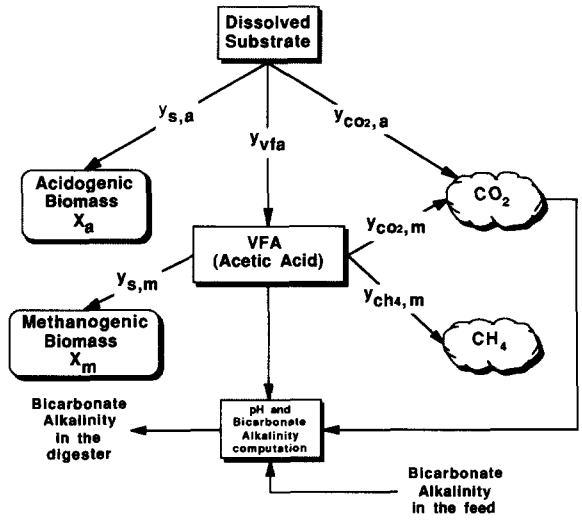

Fig. 2. Interactions at the basis of the simplified model showing the yield factors controlling the conversion from one stage to another.

The model assumes that the substrate is available in dissolved form and is partly converted into acidogenic cells through $y_{s,a}$ yield factor and partly acidified through y_{vfa}, whereas the remaining fraction yields CO_2. Likewise, acetic acid yields both carbon dioxide and methane through $y_{co2,m}$ and y_{ch4} respectively, and only part of it is taken up by methanogens through $y_{s,m}$.

Now that the basic connections have been established, the model equations can be derived. As a first step the hydraulic regime has to be defined. Based on a number of tracer experiments, the reactor where the anaerobic digestion process takes place, an anaerobic filter with recycle, can be approximated by a completely stirred tank reactor (CSTR). This implies that each dynamic equation has, in addition to the kinetic terms, an input/output mass balance which depends on the dilution rate $D = F/V$, where F is the liquid volumetric flow and V the volume of the liquid phase. The organisms in the vessel are attached to the inert packing medium and cannot move freely. Thus the hydraulic and solids dilution rates will greatly differ and this is accounted for in writing the appropriate mass balance equations for the bacteria. The solid dilution rate D' is expressed as a fraction δ of the hydraulic dilution

rate D, namely $D' = \delta D = \delta F/V$, with $0 < \delta < 1$. For the control of alkalinity, a source of alkali (sodium bicarbonate in this case) is added into the feed tank prior to entering the digester. Therefore it follows the same transport dynamics as the main process stream, i.e. the organic load, and the hydraulic regime of the reactor applies equally to both inputs. Hence the sodium bicarbonate actually entering the digester (B) has the following dynamics

$$\frac{dB}{dt} = D(B_{in} - B) \quad (2.1)$$

The model has six dynamic variables: organic substrate, acidogenic and methanogenic bacteria, acetic acid, and carbon dioxide both the liquid and gas phases. Now the dynamics of each of them is considered.

2.1. Organic substrate (S)

It is assumed that the input to the system is composed of organic biodegradable matter in dissolved form, ready to be processed by acidogenic bacteria. Thus the dynamics for substrate transformation is composed of a mass transfer and an acidogenic bacteria-based (X_a) conversion term. Given the CSTR assumption the first is given by the difference between incoming (S_{in}) and outgoing (S) substrate multiplied by the dilution rate D. For the biological term, a modified Monod kinetics is used with three separate yield factors relative to substrate conversion into acidogenic bacteria ($y_{s,a}$), volatile fatty acids (y_{vfa}) and CO_2 ($y_{co2,a}$) respectively

$$\frac{dS}{dt} = D(S_{in} - S) - \frac{\mu_{a,max} S}{K_{s,a} + S} \cdot \frac{S_{in} + K_{s,a}}{S_{in}} \cdot X_a \cdot \left(\frac{1}{y_{s,a}} + y_{vfa} + y_{co2,a} \right) \quad (2.2)$$

The idea of using three separate yield factors may appear uncanny, but in fact they sum up to a single number and in this way the various pathways of substrate degradation can be kept conceptually separated. The additional term to the Monod kinetics $(S_{in} + K_{s,a})/S_{in}$ was introduced in order to establish a proportionality between the half-velocity constant $K_{s,a}$ and the incoming substrate, as suggested by Pavlostatis and Giraldo-Gomez (1991).

2.2. Acidogenic bacteria (X_a)

This kinetics is related to the previous mechanism of substrate utilization, save for the fact that no acidogenic bacteria are assumed in the input stream. The rate of organism loss through the output stream is related to the solid dilution rate D' which takes into account the fact that almost all the biomass is retained by being attached to the inert packing material and thus only a small fraction leaves the system. In addition, an endogenous decay term $k_{d,a}$ is introduced.

$$\frac{dX_a}{dt} = \frac{\mu_{a,max} S}{K_{s,a} + S} \cdot \frac{S_{in} + K_{s,a}}{S_{in}} X_a - (k_{d,a} + D') X_a \quad (2.3)$$

2.3. Acetic acid (V_a)

The conversion of carbonaceous substrate into volatile fatty acid (here assumed to be all as acetic acid) is obtained through the acidogenic bacteria. In tailoring the model response to the available data it was found that the most appropriate kinetics for this interaction is a substrate-limited Haldane kinetics (Bailey and Ollis, 1986) with $K_{i,m}$ as the inhibiting factor and $K_{s,a}$ as the half-velocity constant. In this case it is well known (Pavlostatis and Giraldo-Gomez, 1991) that the substrate/inhibiting factor of the methanogens growth rate is the undissociated fraction of volatile fatty acid (acetic acid in this case), which can be computed from the total acid concentration as

$$HAc = V_a \left(1 + \frac{K_a}{[H^+]} \right)^{-1} \quad (2.4)$$

where HAc is the undissociated fraction and V_a the total acetic acid.

The conversion factors are y_{vfa} from substrate to acetic acid and $y_{s,m}$ from acetic acid into acidogenic bacteria, y_{co2} and y_{ch4} into CO_2 and CH_4 gas respectively, as shown in Fig. 2. The

acetic acid dynamics includes a depletion term due to the utilization by methanogens. The complete acetic acid dynamics is then

$$\frac{dV_a}{dt} = D \cdot (V_{a_{in}} - V_a) + \frac{\mu_{a,max} S}{K_{s,a} + S} \cdot \frac{S_{in} + K_{s,a}}{S_{in}} X_a \cdot y_{vfa} - \frac{\mu_{m,max} X_m}{1 + \frac{K_{s,m}}{HAc} + \frac{HAc}{K_{i,m}}} \cdot \left(\frac{1}{y_{s,m}} + y_{co2,m} + y_{ch4} \right) \quad (2.5)$$

2.4. Methanogenic bacteria (X_m)

Their dynamics is governed by the decomposition of the undissociated fraction of acetic acid (HAc) which plays the double role of substrate/inhibitor. As with the acidogenic bacteria X_a it is supposed that no bacteria are carried in through the liquid input stream.

$$\frac{dX_m}{dt} = \frac{\mu_{m,max} X_m}{1 + \frac{K_{s,m}}{HAc} + \frac{HAc}{K_{i,m}}} - (D' + k_{d,m}) \cdot X_m \quad (2.6)$$

2.5. Carbon dioxide (C)

This dynamics is the most complex of the whole system, because it relates the reactions in the liquid phase with the composition of the gas and this in turn affects the pH balance in the liquid. This is also important in view of bicarbonate alkalinity (BA) modelling, as will be shown in the next section.

The production of CO_2 depends on the activity of both microbial compartments X_a and X_m through yield coefficients $y_{co2,a}$ and $y_{co2,m}$ respectively, plus a term responsible for the rate of CO_2 mass transfer through $K_L a$ between the liquid and the gas phase, according to Henry's law. Thus the complete CO_2 dynamics is

$$\frac{dC}{dt} = -D \cdot C + \frac{\mu_{a,max} S}{K_{s,a} + S} \cdot \frac{S_{in} + K_{s,a}}{S_{in}} \cdot X_a \cdot y_{co2,a} + \frac{\mu_{m,max}}{1 + \frac{K_{s,m}}{HAc} + \frac{HAc}{K_{i,m}}} \cdot X_m \cdot y_{co2,m} + K_L a \cdot (K_h \cdot P_{co2} - C) \quad (2.7)$$

2.6. Carbon dioxide partial pressure (P_{co2})

This depends on two terms: the first is the exchange of CO_2 between the liquid and gas phase, multiplied by the total pressure in the gas phase P_t. In this expression $K_h P_{co2}$ represents the CO_2 saturation value in the liquid and $K_L a$ the gas transfer rate. The second term represents the CO_2 loss with the gas output flowrate Q.

$$\frac{dP_{co2}}{dt} = -P_t \left(\frac{S_v \cdot V}{C_{co2} \cdot V_g} \right) \cdot K_L a \cdot (K_h \cdot P_{co2} - C) - \left(\frac{Q}{V_g} \right) P_{co2} \quad (2.8)$$

where S_v is Avogadro's constant, C_{co2} is the conversion factor from mole to mg l^{-1} for carbon dioxide, V is the total digester volume and V_g the gas volume.

2.7. Gas production

It can be computed from the previous dynamic balance. In fact the gas flow rates of carbon dioxide and methane are controlled by the difference of partial pressures in the two phases

$$Q_{co2} = -\left(\frac{S_v \cdot V}{C_{co2}} \right) \cdot K_L a \cdot (K_h \cdot P_{co2} - C) \quad (2.9)$$

where the minus sign is consistent with the fact that the balance is written for the liquid phase, therefore the outgoing gas flow is a negative contribution since it leaves the system.

The rate of conversion of acetic acid into methane by means of the methanogenic bacteria is assumed to be proportional to their growth rate

$$Q_{ch4} = \frac{S_v \cdot V}{C_{ch4}} \frac{\mu_{m,max}}{1 + \frac{K_{s,m}}{HAc} + \frac{HAc}{K_{i,m}}} \cdot X_m \cdot y_{ch4} \tag{2.10}$$

where C_{ch4} is the conversion factor from mole to mg l^{-1} for methane.

3. Determination of pH and alkalinity

An algorithm is now developed to determine the alkalinity in the liquid phase. It originates from basic ion balance and a two-phase system is considered to take into account the liquid/gas equilibrium. Carbon dioxide in both phases is considered and alkalinity is expressed as sodium bicarbonate molarity.

3.1. CO_2 equilibrium

The CO_2 balance between the two phases is governed by Henry's law

$$K_h = \frac{CO_{2(aq)}}{CO_{2(g)}} \tag{3.1}$$

In the liquid phase the dissolved $CO_{2(aq)}$ is present as carbonic acid with the following equilibrium

$$K_{co2} = \frac{[H^+][HCO_3^-]}{H_2CO_3} = 4.5 \times 10^{-7} \tag{3.2}$$

Considering partial dissociation of $CO_{2(g)}$ yields

$$\begin{aligned}[H_2CO_3] &= K_h CO_{2(g)} \\ &= [HCO_3^-] + \frac{[H^+][HCO_3^-]}{K_{co2}} \\ &= [HCO_3^-]\left(\frac{[H^+]}{K_{co2}} + 1\right)\end{aligned} \tag{3.3}$$

Assuming that all the cations $[H^+]$ come from the dissociation of H_2CO_3, the electroneutrality condition yields

$$[H^+] = [HCO_3^-] \tag{3.4}$$

therefore Eq. 3.3 yields

$$[H^+]^2 + K_{co2}[H^+] - K_h K_{co2} CO_{2(g)} = 0 \tag{3.5}$$

A simplified version can be obtained supposing that all the $CO_{2(g)}$ translates into what can be indicated as H_2CO_3 and this is partially dissociated. Substituting Eq. 3.1 in Eq. 3.2 and solving for HCO_3^- yields

$$[HCO_3^-] = \frac{K_h K_{co2} CO_{2(g)}}{[H^+]} \tag{3.6}$$

where $CO_{2(g)}$ is expressed as gas partial pressure [atm]. Applying Eq. 3.4 again and solving for $[H^+]$ yields

$$[H^+]^2 = K_h K_{co2} CO_{2(g)} \tag{3.7}$$

This approximation will be used throughout in the paper.

3.2. pH of a solution containing a weak acid

If a weak acid is present (e.g. acetic acid, CH_3COOH), its dissociation can be accounted for through the solubility product

$$K_a = \frac{[H^+][A^-]}{[HA]} \tag{3.8}$$

In addition the water ion product is considered

$$K_w = [H^+][OH^-] = 10^{-14} \tag{3.9}$$

and the electroneutrality condition yields

$$[H^+] = [A^-] + [OH^-] \tag{3.10}$$

If the acid mass balance is considered, where HA_o is the total acid mass,

$$\begin{aligned}[HA_o] &= \frac{[H^+][A^-]}{K_a} + [A^-] \\ &= [A^-]\left(\frac{[H^+]}{K_a} + 1\right)\end{aligned} \tag{3.11}$$

computing the $[A^-]$ concentration from Eq. 3.10 and substituting in Eq. 3.11 yields

$$[HA_o] = \left([H^+] - \frac{K_w}{[H^+]}\right)\left(\frac{[H^+]}{K_a} + 1\right) \quad (3.12)$$

Rearranging and solving for $[H^+]$ yields the following third-order equation

$$[H^+]^3 + K_a[H^+]^2 - (K_w + K_aHA_o)[H^+] - K_wK_a = 0 \quad (3.13)$$

3.3. Inclusion of CO_2 partial pressure

Carbon dioxide diffusion in the liquid phase and consequent acidification is now considered. The difference with the previous case is that more HCO_3^- anions are generated through the dissolution of gaseous CO_2. Thus the electroneutrality condition becomes

$$[H^+] = [A^-] + [OH^-] + [HCO_3^-] \quad (3.14)$$

solving for $[A^-]$ and substituting the expressions of the various anions in terms of $[H^+]$ yields

$$[A^-] = [H^+] - \frac{K_w}{[H^+]} - \frac{K_{co2}K_wCO_{2(g)}}{[H^+]} \quad (3.15)$$

Substituting in the acid mass balance (Eq. 3.10) yields

$$[HA_o] = \left([H^+] - \frac{K_w}{[H^+]} - \frac{K_hK_{co2}CO_{2(g)}}{[H^+]}\right) \times \left(\frac{[H^+]}{K_a} + 1\right) \quad (3.16)$$

Rearranging and solving for $[H^+]$ yields

$$[H^+]^3 + K_a[H^+]^2 - (K_w + K_a[HA_o] + K_hK_{co2}CO_{2(g)})[H^+] - (K_w + K_hK_{co2}CO_{2(g)})K_a = 0 \quad (3.17)$$

3.4. Addition of other input ionic species

To extend the model applicability to a number of different shock conditions, the case when the loading comes from an excess of acetic species in the input, either in the form of acetate (sodium acetate or sodium hydroxide) or of acetic acid, is now considered. This reflects in the coefficients of the ion balance equation used to compute pH and alkalinity. Assuming the same dissociation constant for all the acetic acid species, the acid mass balance becomes

$$[HA_o] = \frac{[H^+][A^-]_{HAc+NaAc}}{K_a} + [A^-]_{HAc+NaAc} \quad (3.18)$$

The electroneutrality condition, taking all sodium ions into account, becomes

$$[H^+] + [Na^+]_{bic} + [Na^+]_{NaAc} = [A^-]_{HAc+NaAc} + [OH^-] + [HCO_3^-] \quad (3.19)$$

where the subscripts 'bic', 'NaAc' and 'HAc' refer to the ions introduced by sodium bicarbonate, sodium acetate and acetic acid respectively. As a result the ion balance equation has the same structure as before, but now the coefficients of the $[H^+]^2$ and $[H^+]$ terms depend on all the ion species in the system, namely

$$[H^+]^3 + (K_a + [Na^+]_{bic} + [Na^+]_{NaAc})[H^+]^2 - (K_a([HAc_o] - [Na^+]_{bic} - [Na^+]_{NaAc}) + K_w + K_hK_{co2}CO_{2(g)})[H^+] - K_a(K_w + K_hK_{co2}CO_{2(g)}) = 0 \quad (3.20)$$

It can easily be demonstrated that Eq. 3.20 has only one feasible root, which is precisely the $[H^+]$ concentration in the system.

4. Steady-state model solution

The previous equations describe the behaviour of the process under dynamic conditions, but in many cases it is also important to determine the steady-state which the system would eventually reach when its operating conditions are kept constant in time. Further, steady-state analysis is a powerful tool to determine the influence that inputs have on process conditions and how the most suitable operating point can be determined

by adjusting them. The steady-state solution of the model can be obtained by long-term simulation, but this is an awkward and time-consuming procedure, whereas it can be readily obtained by setting the time derivatives of Eqs. 2.2–2.8 to zero and solving for the process variables. Chain substitution can be applied only to a limited extent because of the feedback link between pH and the undissociated fraction of acetic acid, HAc.

It is straightforward to work out the steady-state acidogenic stage setting to zero the time derivatives of Eqs. 2.2–2.4 and solving for X_a, S and HAc respectively. Eq. 2.3 can be solved for the substrate

$$S = \frac{K_{s,a}(D' + K_{d,a})}{\mu_{a,max}\left(\frac{S_{in} + K_{s,a}}{S_{in}}\right) - K_{d,a} - D'} \tag{4.1}$$

This is substituted in Eq. 2.2, which is then solved for the acidogenic bacteria X_a

$$X_a = \frac{D\cdot(S_{in} - S)}{\left[\mu_{a,max}\frac{S_{in} + K_{s,a}}{S_{in}}\cdot\frac{S}{K_{s,a} + S}\right]\cdot\left(y_{vfa} + y_{co2,a} + \frac{1}{y_{s,a}}\right)} \tag{4.2}$$

Solving Eq. 2.5 for the undissociated acetic acid fraction yields the quadratic equation

$$\mathrm{HAc}^2 - \frac{K_{i,m}(\mu_{m,max} - D' - K_{d,m})}{D' + K_{d,m}}\cdot\mathrm{HAc} + K_{i,m}\cdot K_{s,m} = 0 \tag{4.3}$$

from which the total acetic acid can be determined using Eq. 2.4 in reverse

$$V_a = \mathrm{HAc}\left(1 + \frac{K_a}{[\mathrm{H}^+]}\right) \tag{4.4}$$

The concentration of methanogens can be obtained from Eq. 2.6 since HAc is now known

$$X_m = \frac{D(V_{a,in} - V_a) + y_{co2,a}\left[\mu_{a,max}\frac{S_{in} + K_{s,a}}{S_{in}}\cdot\frac{S\cdot X_a}{K_{s,a} + S}\right]}{\mu_{m,max}\Big/\left(1 + \frac{K_{s,m}}{\mathrm{HAc}} + \frac{\mathrm{HAc}}{K_{i,m}}\right)} \tag{4.5}$$

The methane gas production rate can then be computed through Eq. 2.10. So far the computation has been rather straightforward, save for the pH appearing in the acetic acid equation (Eq. 4.4). Since pH is determined from the carbonate equilibrium across the phases, the CO_2 balance must be solved and pH determined in an iterative way. To do this the CO_2 partial pressure is determined solving Eqs. 2.7–2.8 for P_{co2} and C. Some substitutions and rearrangements yield the following second-order algebraic equation for P_{co2}

$$aDK_L aK_h P_{co2}^2 - [a\cdot K_L a(\alpha + \delta + DK_h) + Q_{ch4}(D + K_L a)]\cdot P_{co2} + a\cdot K_L a(\alpha + \delta) = 0 \tag{4.6}$$

where

$$a = \frac{S_v\cdot V}{C_{co2}}$$

$$\alpha = \frac{\mu_{a,max}\cdot S}{K_{s,a} + S}\cdot\frac{S_{in} + K_{s,a}}{S_{in}}\cdot X_a\cdot y_{co2,a} \tag{4.7}$$

$$\delta = \frac{\mu_{m,max}\cdot X_m}{1 + \frac{K_{s,m}}{\mathrm{HAc}} + \frac{\mathrm{HAc}}{K_{i,m}}}\cdot y_{co2,m}$$

Once Eq. 4.6 is solved the CO_2 content in the liquid phase can be obtained by direct substitution into Eq. 2.7

$$C = \frac{\alpha + \delta + K_h\cdot K_L a\cdot P_{co2}}{D + K_L a} \tag{4.8}$$

Now that both V_a and P_{co2} are available, the pH computation is iterated, using a bisection algorithm, until a solution is found to a given tolerance. This completes the determination of the digester steady-state.

Using typical values for the kinetic constants, this stationary model was used to determine how the inputs influence the system. Three control variables were selected: input organic load (S_{in}), input bicarbonate (BA_{in}) and dilution rate (D). The first should be regarded as a disturbance, since no control over it can be exerted. Likewise, the third cannot be varied because the digester design is fixed and the feed usually cannot be altered since the amount of wastewater to be treated is fixed. In this sense the steady-state model can assist in the design by selecting the

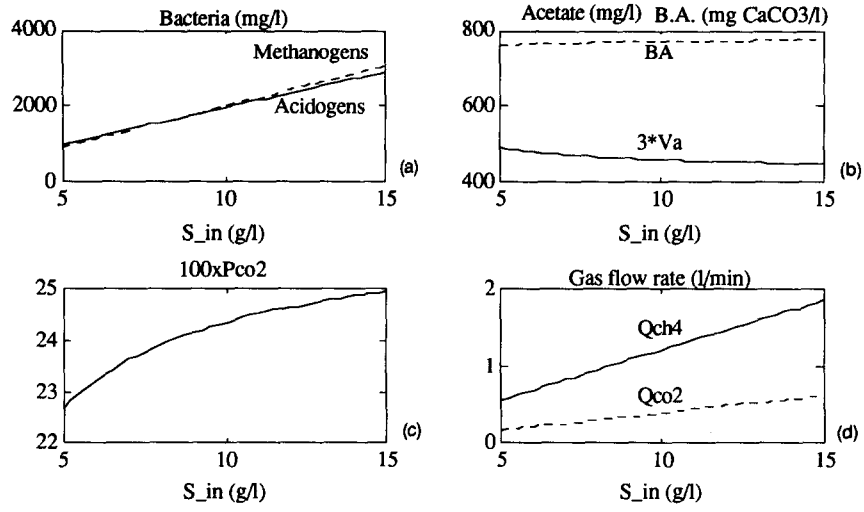

Fig. 3. Effect of the stationary level of organic load S_{in} on the process variables.

most appropriate dilution rate for the required process specifications. The only input variable suitable for real-time control, especially during organic loading shocks, is the input bicarbonate which can be used to control the pH and the bicarbonate alkalinity in the digester.

Figs. 3, 4 and 5 show how the steady-state of the system is altered by changing each input variable.

Considering Fig. 3, which shows the effect of varying the input organic substrate, it is interesting to notice that the process is little affected by

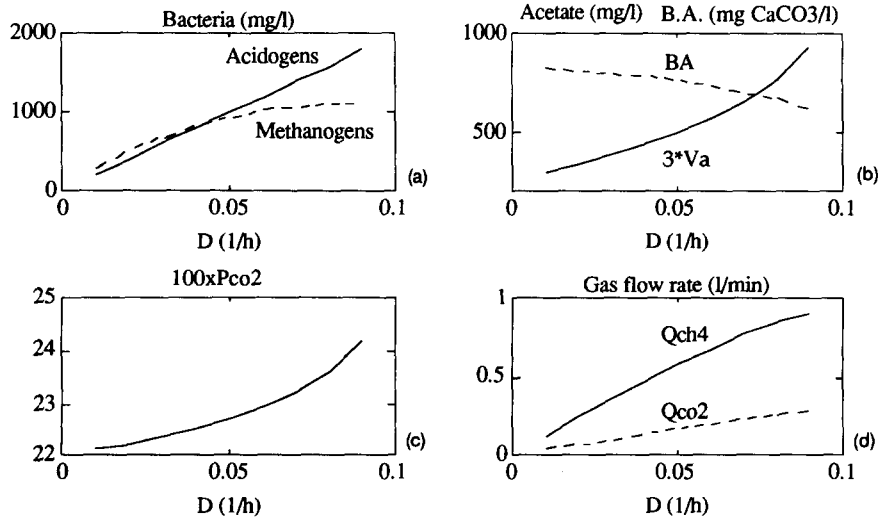

Fig. 4. Effect of the stationary level of the dilution rate on the process variables.

its level, provided that the load is stationary. The most notable effect is the almost linear growth of both bacterial populations (Fig. 3a) and the slight decrease of acetate (Fig. 3b). Here the value of the acetate V_a is multiplied by a factor of 3 in order to fit in the same graph with bicarbonate alkalinity (BA). Comparing these responses with the shock behaviours shown in the following sections, a striking difference emerges, though the values considered in the two approaches are almost the same. The organic loading shock produces a dramatic change in the short time scale. In fact during the shock the increased production of acetic acid due to acidification of the excess substrate is not balanced by an equal uptake rate by the following methanogenic phase. The temporary glut of acetic acid determines the decrease of bicarbonate alkalinity and the increase of CO_2, which is produced directly from the acidogenic stage. As a consequence both CO_2 partial pressure (Fig. 3c) and gas production (Fig. 3d) increase.

The variation of the dilution rate D is considered in Fig. 4. In the context of shock loading control, this has a very limited significance, since with anaerobic digesters the dilution rate is primarily a design parameter, as the feed rate usually cannot be varied during operation. However, as far as bacterial populations are concerned (Fig. 4a), an increase of dilution rate affects the acidogens more than the methanogens, for which a saturation occurs. The acetate increases with the dilution rate, but the bicarbonate alkalinity decreases (Fig. 4b), whereas both CO_2 and CH_4 flowrates increase with D. However, the increase is not the same for all quantities and the increase of D seems to privilege the acidic phase with more acetate being present and hence more CO_2 being produced.

Referring now to Fig. 5, the input bicarbonate is increased. As a result, the system pH increases and so does the acetate. The reason for this can be explained by Eq. 4.4. Since the undissociated fraction HAc is fixed by the kinetic parameters alone, decreasing the $[H^+]$ causes an increase in V_a. The effect on the bacterial populations is quite marked: though the acidogens are unaffected by the change, the methanogens decline considerably and are no longer capable of eliminating the available acetic acid, with the result of an acetate build up. At the same time the bicarbonate alkalinity increases too as a result of the increasing alkalinity entering the system (Fig. 5b). This results in a linear increase in CO_2 (Fig. 5c), whereas the gas production is almost unaffected by this (Fig. 5d).

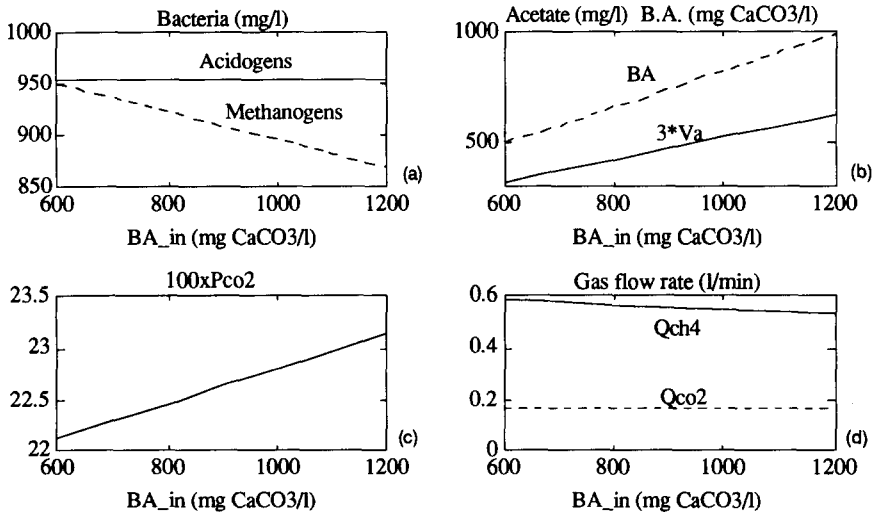

Fig. 5. Effect of the stationary level of input bicarbonate BA_{in} on the process variables.

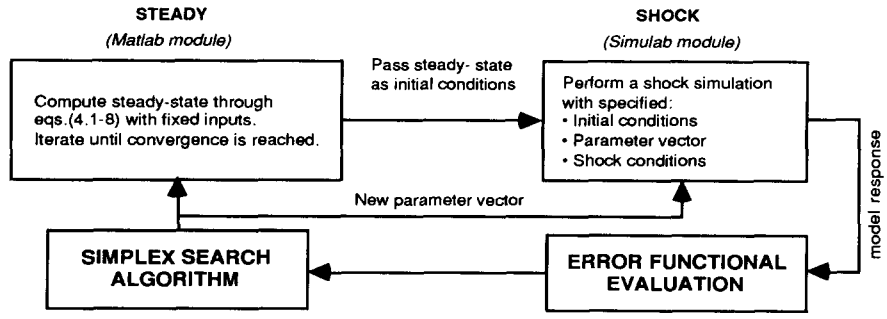

Fig. 6. Organization of SIMULAB modules in conjunction with the search algorithm, to solve the problem of initial conditions sensitivity.

5. Parameter calibration

Once the model structure is specified, the numerical values of its parameters have to be estimated in such a way that the weighted sum of squared errors between the set of N_{exp} experimental observations and the corresponding set of model outputs is a minimum for a unique value $\boldsymbol{P}^*$ of the parameter vector. The available experimental quantities were bicarbonate alkalinity (BA) and CO_2 partial pressure in the output gas (P_{co2}). Thus the error functional used in the calibration takes the form of the sum of the squared errors between experimental data and corresponding model outputs for these two variables

$$\boldsymbol{P}^* = \min_{\boldsymbol{P}} E(\boldsymbol{P})$$

$$= \min_{\boldsymbol{P}} \sum_{i=1}^{N_{exp}} \left\{ \left[\mathrm{BA}^i_{\mathrm{m}}(\boldsymbol{P}) - \mathrm{BA}^i_{\mathrm{exp}} \right]^2 + \left[P^i_{\mathrm{co2m}}(\boldsymbol{P}) - P^i_{co2\mathrm{exp}} \right]^2 \right\} \qquad (5.1)$$

with model equations 2.2–2.10 acting as constraints. Thus parameter estimation generates an optimization problem where the objective functional is the squared error sum $E(\boldsymbol{P})$ and the decision variables are the p components of the parameters vector $\boldsymbol{P}$. Two main difficulties arise in conjunction with the optimization problem (Eq. 5.1). Firstly, for many complex system no analytical solution is available. Secondly, the correlation among model parameters may produce an elongated error functional whose minimum is numerically difficult to determine.

For these reasons the parameter estimation problem has been pursued through a numerical approach. The computational scheme involves three main steps:

1 Numerical simulation of system dynamics with a given set of parameters $\boldsymbol{P}$
2 Evaluation of the corresponding error functional $E(\boldsymbol{P})$
3 Computation of an improved estimate of the parameter vector $\boldsymbol{P}$ in terms of a decreasing $E(\boldsymbol{P})$ through the numerical search algorithm based on an optimized version of the classical Nelder and Mead flexible polyhedron search.

Table 1
Organic loading shock experimental conditions

	Experiment 1, calibration		Experiment 2, validation	
	Baseline	Shock (8 h)	Baseline	Shock (8 h)
Feed (mg COD/l)	4670	9130	4468	12470
OLR (kg COD/m^{3}d)	9.7	18.9	9.271	26.9
Recycle rate (ml/min)	20		20	
Influent flow rate (l/min)	0.481		0.481	

Table 2
Model parameter values

Symbol		Value	Units	Purpose
Kinetic constants				
$\mu_{a,max}$	L [a]	0.5033	h^{-1}	Acidogenic bacteria maximum growth rate
$K_{s,a}$	C	238.1 ± 3.7	$mg\,l^{-1}$	Acidogenic bacteria half-velocity
$K_{d,a}$	C	0.03104 ± 0.000484057	h^{-1}	Acidogenic bacteria decay rate
$\mu_{m,max}$	C	0.00227 ± 9.6834e − 06	h^{-1}	Methanogenic bacteria maximum growth rate
$K_{s,m}$	C	0.01453 ± 0.000226874	$mg\,l^{-1}$	Methanogenic bacteria half-velocity
$K_{d,m}$	L	0.0008	h^{-1}	Methanogenic bacteria decay rate
$K_{i,m}$	C	35.47 ± 0.4923	$mg\,l^{-1}$	Methanogenic bacteria inhibition conc.
Yield coefficients				
$y_{s,a}$	L	0.688		Substrate → acidogenic bacteria
y_{vfa}	L	0.427		Substrate → acetic acid
$y_{co2,a}$	C	0.5 ± 0.00704515		Substrate → CO_2
$y_{s,m}$	L	3.2702		Acetic acid → acidogenic bacteria
y_{ch4}	L	20.7321		Acetic acid → methane
$y_{co2,m}$	C	5.174 ± 0.4923		Acetic acid → CO_2
Physico-chemical constants and reactor design parameters				
K_w	L	1×10^{-14}		Water dissociation constant
C_{co2}	L	44 000		mole → $mg\,l^{-1}$ conv. const. for CO_2
C_{ch4}	L	16 000		mole → $mg\,l^{-1}$ conv. const. for CH_4
P_t	E	1	atm	Total pressure in the gas phase
V	E	10	l	Liquid phase volume
V_g	E	2.5	l	Gas phase volume
F	E	0.48	$l\,h^{-1}$	Liquid flow rate
δ	E	0.01666	–	Liquid/solid dilution rate ratio
$K_L a$	C	6.382 ± 0.100045	h^{-1}	CO_2 mass transfer rate coefficient

[a] C = calibrated; E = Experimental condition; L = literature.

These three steps are iterated until a "satisfactory" parameter vector $\boldsymbol{P}^*$ is found. The details of the search procedure are summarized in the following block diagram. The algorithmic details of the search method are described in Marsili-Libelli and Castelli (1987) and its application to biotechnological models is considered in Marsili-Libelli (1992). This method represents an extension of the approach described by Richter and

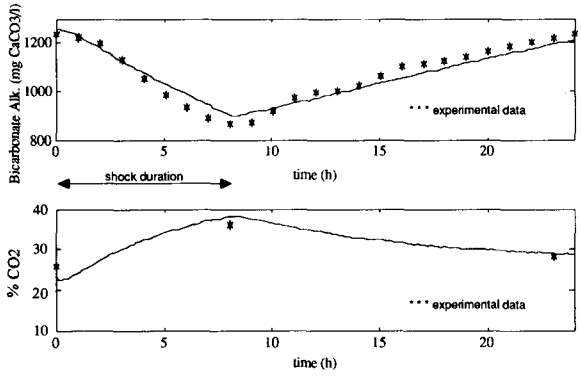

Fig. 7. Comparison of model response and data set from Experiment 1 of Table 1.

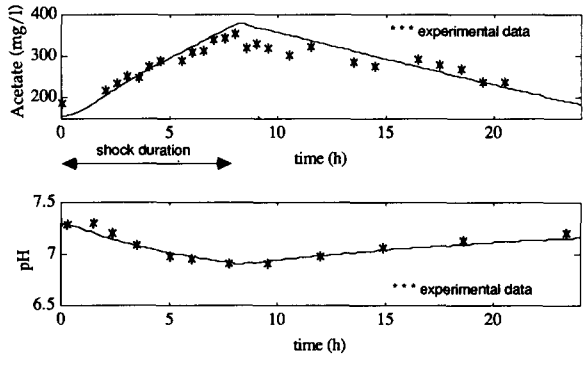

Fig. 8. Additional comparison of model response and data set from Experiment 1 of Table 1.

Table 3
Parameter correlation matrix

	$K_{s,a}$	$K_{d,a}$	$\mu_{m,max}$	$K_{s,m}$	$K_{i,m}$	$y_{co2,m}$	$y_{co2,a}$	$K_L a$
$K_{s,a}$	1.0000	0.0102	−0.0116	0.0001	−0.0024	−0.0080	−0.0081	0.0019
$K_{d,a}$	0.0102	1.0000	−0.0031	0.0001	0.0007	−0.0023	−0.0025	0.0009
$\mu_{m,max}$	−0.0116	−0.0031	1.0000	0.0077	−0.1134	−0.2059	−0.1799	0.0058
$K_{s,m}$	0.0001	0.0001	0.0077	1.0000	0.0022	0.0054	0.0042	0.0018
$K_{i,m}$	−0.0024	0.0007	−0.1134	0.0022	1.0000	−0.1171	−0.1107	0.0006
$y_{co2,m}$	−0.0080	−0.0023	−0.2059	0.0054	−0.1171	1.0000	−0.1651	−0.0031
$y_{co2,a}$	−0.0081	−0.0025	−0.1799	0.0042	−0.1107	−0.1651	1.0000	−0.0049
$K_L a$	0.0019	0.0009	0.0058	0.0018	0.0006	−0.0031	−0.0049	1.0000

Söndgerath (1990) and Seber and Wild (1989). The digester model equations 2.2–2.10 were implemented using SIMULAB® graphic simulation language and the pH equation 3.20 was included as a separate MATLAB® module. The supervising optimization procedure was also written in MATLAB® language and the whole system was run on a Macintosh IIci.

In this application, it was observed that the model is very sensitive to initial conditions, which are in principle unknown and depend on the parameter values. To minimize the effect of this undesirable coupling the calibration procedure was organized iteratively as shown in Fig. 6.

As already stated in the introduction, the experimental data used for both calibration and validation came from shock experiments supplied by the University of Glamorgan. They were obtained from the laboratory reactor and the bicarbonate alkalinity monitor described in Hawkes et al., 1993. Two process variables were measured: bicarbonate alkalinity (BA) and CO_2 partial pressure (P_{co2}). The pilot digester design was an anaerobic filter with recycle and the experiments consisted of applying an 8-h organic load shocks over a quasi steady-state baseline of nearly 4500 mg COD/l for approximately 24 h. The exact experimental conditions are summarized in Table 1.

5.1. Calibration results

The model has a large number of parameters, some of which are known in principle as they are available from the general knowledge of physical chemistry (e.g. K_h, Henry's constant for CO_2) were not included in the calibration. Others are specific to this model and were estimated on the basis of experimental data. The following is the list of all the model parameters, either calibrated with the above procedure or obtained by other means as indicated in the second column of Table

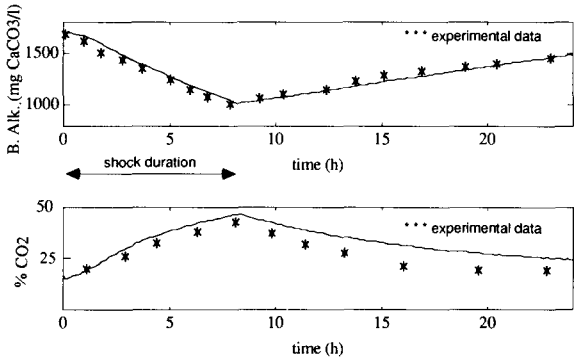

Fig. 9. Model validation with the data from Experiment 2 of Table 1.

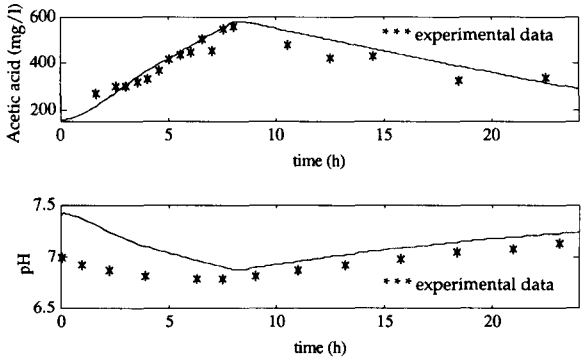

Fig. 10. Additional model validation with the data from Experiment 2 of Table 1.

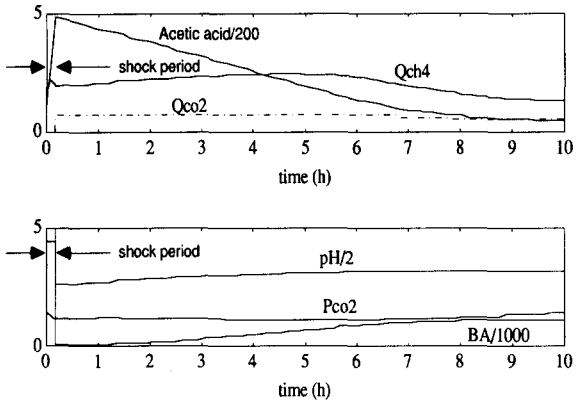

Fig. 11. Model response to an acetic acid shock specified as in Fig. 2a.

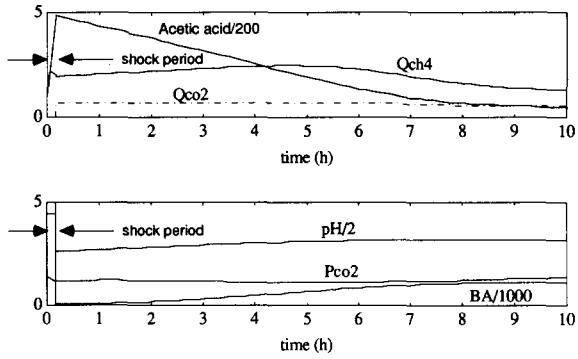

Fig. 13. Model response to the sodium acetate shock specified as Fig. 2b.

2. For the calibrated parameters (marked with 'C' in the second column) the confidence interval of the estimate is also given.

The parameter correlation matrix was also computed (Table 3). This gives an appreciation of the correlation between paired parameters. It can be seen that all off-diagonal terms are much smaller than 1 in absolute value. This means that the interaction between parameters, i.e. their structural redundancy in the model is very limited.

With these numerical values the agreement between experimental data obtained from experiment 1 in Table 1 and model response shown in Fig. 7 were obtained. The 8-h shock begins at time 0 and its duration is indicated in the diagrams. It can be seen that after the shock the system tends to recover the original steady state.

With the calibrated model, more simulations were produced in order to assess how the model could reproduce some other process variable for which experimental data were available, but were not used in the calibration. Acetic acid and pH were selected as relevant and the agreement between model and data are shown in Fig. 8. No further parameter adjustments were made in this simulation.

5.2. Model validation

To assess the validity of the previous calibration results, the model with these parameter values was run again and its output compared with the data obtained from the experiment 2 in Table

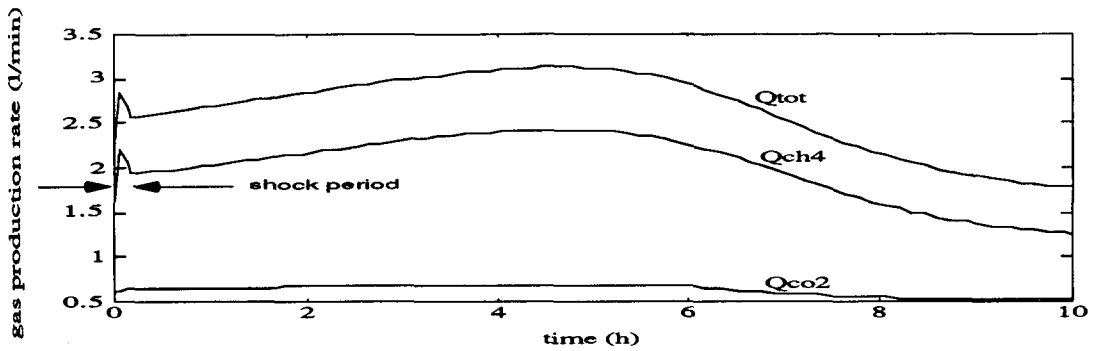

Fig. 12. Acetic acid shock: effect on gas production rate.

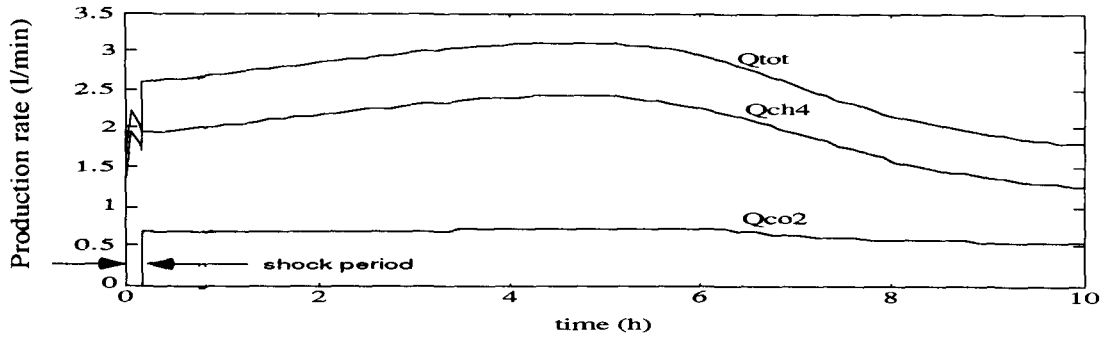

Fig. 14. Sodium acetate shock: effect on gas production rate.

1 representing an unrelated shock experiment, without altering the parameter values obtained in the previous run. The results of this validation run are shown in Figs. 9 and 10.

In the last graph some discrepancy between observed and simulated pH is observed, possibly because of some unspecified buffering action which the model does not include.

6. Shock experiments

So far the shocks were considered to originate from organic overloading only. Now with the calibrated model some further shock experiments can be simulated, including disturbances concerning the acidic stage. While the sizing and dilution rate of the digester remained unchanged, the new shock conditions for the feed were defined as follows

1 *Base conditions*:
   a Organic loading: constant at 10 000 mg COD/l
   b Sodium bicarbonate: constant at 800 mg $CaCO_3$/l
2 *Shock inputs*:
   a Acetic acid shock: 82 000 mg/l as HAc for 0.17 h (nearly 10 min)
   b Sodium acetate shock: 82 000 mg/l as NaAc for 0.17 h (nearly 10 min)

The model responses are shown in Figs. 11–14.

The effect of the two shocks is about the same. Since a large amount of acetic acid is made available, the acidogenic phase is largely bypassed and the methanogenic phase can proceed more quickly. In fact the methane production rate increases whereas the acetic acid in the system is consumed. Likewise, the pH decreases sharply during the shock and takes a long time to go back to the original level. The bicarbonate alkalinity is severely decreased by the shock and takes a considerable amount of time to rise back to its original level. Its trend is almost exactly opposite to the acetic acid behaviour. All the variables seem to act with almost the same time constant and stabilise in about 10 h. The interesting fact is that it seems that these are permanently affected by the shock and do not return to their pre-shock values.

7. Alkalinity feedback control through bicarbonate dosing

The model was ultimately conceived for the control of the bicarbonate dosing system in conjunction with the new BA monitoring system (Hawkes et al., 1993). This action is particularly

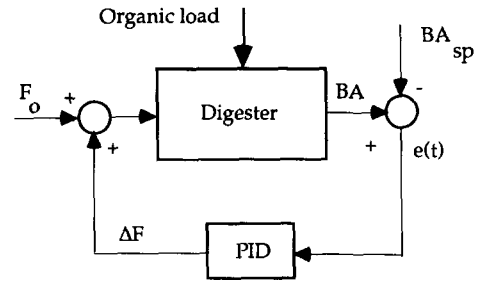

Fig. 15. Scheme of the alkalinity feedback controller.

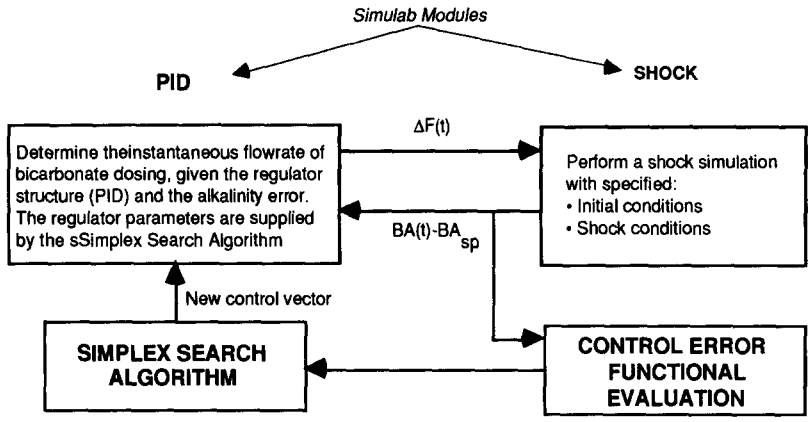

Fig. 16. Computational scheme for the optimization of the PID controller parameters.

important to protect the digester from the adverse effects of sudden loading shocks. The control scheme of Fig. 15 considers the manipulation of sodium bicarbonate flowrate in response to the error signal between the desired alkalinity value and its actual value given by the BA instrument. A proportional-integral-derivative (PID) regulator was chosen as a feedback controller for its wide availability in the process control industry and the well-tested tuning procedures (Åström and Wittenmark, 1984; Åström and Hägglund, 1988).

Among the many procedures available for PID tuning, an optimal one was chosen (Marsili-Libelli, 1981), since this could be perused in a similar way as the previous parameter calibration problem, with which there are fundamental similarities. In fact both problems reduce to a unique optimization algorithm once an objective functional is defined and the given model is used as a constraint. In the PID controller case the optimization problem can be stated as follows

$$\min_{K_p,T_i,T_d} E_{PID} = \lim_{T\to\infty} \int_0^T \left(BA(t) - BA_{sp}\right)^2 dt \quad (7.1)$$

where K_p, T_i and T_d are the three PID parameters, representing the proportional gain, the reset period and the derivative constant respectively. The optimization procedure determines the controller parameters in such a way that the error functional 7.1 is minimized over the control horizon T. From the computational point of view, the

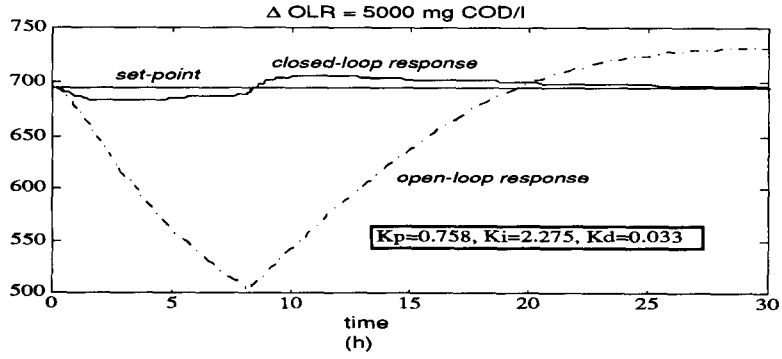

Fig. 17. Organic loading rate shock response of the PID-controlled digester.

control optimization used the previous shock model, in conjunction with the optimization algorithm used for parameter calibration. The only difference is in the objective function E_{PID} instead of $E(\boldsymbol{P})$ and $\{K_p, T_i, T_d\}$ instead of the model parameters. The new computational arrangement is as in Fig. 16.

With this scheme the following controller tuning was obtained for different values of the organic loading shock. Four settings were considered: three of them are on the positive side (increased loading) whereas the fourth consisted of a decreasing load. It was found that the PID tuning obtained for each setting were about the same, thus indicating the wide applicability of this solution. Fig. 17 shows the bicarbonate alkalinity response in the closed-loop arrangement in the case of an overload of 5000 mg COD/l and compares it with the open-loop case. The values of the optimal PID parameters are also listed. It can be seen that the large variation in BA observed in the previous open loop case, both in the simulations and in the experimental data, is substantially diminished through PID control.

8. Conclusion

In this paper a simplified model describing the shock behaviour of an anaerobic digester has been described. It was motivated by the growing interest in digester control through bicarbonate dosing and the recent availability of a new bicarbonate monitoring device. For this reason some features which are normally present in other anaerobic digestion models have been intentionally omitted whereas the emphasis was placed on the system behaviour under shock conditions. The model was implemented using MATLAB/SIMULAB® graphic simulation language and its parameters calibrated with experimental shock data obtained for this purpose. The agreement between data and model response can be considered satisfactory, especially given its simplified structure. The model was then used to simulate other kinds of shock and to assess the design of a bicarbonate dosing PID controller. In both cases the model proved to be a useful tool for process assessment.

Acknowledgements

This research is supported by the European Community grant no. EV5V-CT92-0233 "Integrated Process Control: development of an integrated control system to optimize biological carbon and nitrogen removal by wastewater treatment plants".

The authors also wish to acknowledge the invaluable cooperation of Professor D.L. Hawkes, Dr. F.R. Hawkes and Mr. A.J. Guwy, University of Glamorgan, for supplying the experimental data and for the many helpful discussions and suggestions.

References

Åström, K.J. and Hägglund, T., 1988. Automatic Tuning of PID Controllers. ISA, New York.

Åström, K.J. and Wittenmark, B., 1984. Computer Controlled Systems: Theory and Applications. Prentice Hall, Englewood Cliffs, NJ.

Bailey, J.E. and Ollis, D.F., 1986. Biochemicals Engineering Fundamentals. McGraw-Hill, New York.

Hawkes, F.R., Rozzi, A.G., Black, K., Guwy, A.J. and Hawkes, D.L., 1992. The stability of anaerobic digesters operating on a food-processing wastewaters. Water Sci. Technol., 25: 73–82.

Hawkes, F.R., Guwy, A.J., Rozzi, A.G. and Hawkes, D.L., 1993. A new instrument for on-line measurement of bicarbonate alkalinity. Water Res., 27: 167–170.

Marsili-Libelli, S., 1981. Optimal design of PID regulators. Int. J. Control, 44: 601–616.

Marsili-Libelli, S., 1992. Parameter estimation of ecological systems. Ecol. Model., 62: 233–258.

Marsili-Libelli, S. and Castelli, M., 1987. An adaptive search algorithm for numerical optimization. Appl. Math. Comput., 23: 341–357.

Marsili-Libelli, S. and Nardini, M., 1985. Stability and sensitivity analysis of anaerobic digestion models. Environ. Technol. Lett., 6: 602–609.

McCarthy, P.L. and Mosey, F.E., 1990. Modelling of anaerobic digestion process. Anaerobic treatment technology for municipal and industrial wastewaters. Proc. of the IAWPRC international Specialised Workshop, Valladolid, September 1990, pp. 17–33.

Pavlostatis, S.G. and Giraldo-Gomez, E., 1991. Kinetics of anaerobic treatment: a critical review. Crit. Rev. Environ. Control, 21(5,6): 411–490.

Richter, O. and Söndgerath, D., 1990. Parameter Estimation in Ecology, the Link between Data and Models. VCH VmbH, Weinheim.

Rozzi, A., 1984. Modelling and control of anaerobic digestion processes. Trans. Inst. M. C., 6: 153-159.

Rozzi, A. and Passino, R., 1985. Mathematical Models in Anaerobic Treatment Processes. Mathematical Models in Biological Wastewater Treatment. Elsevier, Amsterdam.

Rozzi, A., Di Pinto, A.C. and Brunetti, A., 1985a. Anaerobic process control by bicarbonate monitoring. Environ. Technol. Lett., 6: 594–601.

Rozzi, A., Merlini, S. and Passino, R., 1985b. Development of a four population model of the anaerobic degradation of carbohydrates. Environ. Technol. Lett., 6: 610–619.

Seber, G.A. and Wild, C.J., 1989. Nonlinear Regression. John Wiley and Sons, New York.

Siegrist, H., Renggli, D. and Gujer, W., 1992. Mathematical modelling of anaerobic mesophilic sewage sludge treatment Int. Symp. on Anaerobic Digestion of Solid Waste, Venice, pp. 53–64.

Van Breusegem, V., Beteau, J.F., Tomei, M.C., Rozzi, A., Cheruy, A. and Bastin, G., 1990. Bicarbonate control strategies for anaerobic digestion process, Proceedings of 11th IFAC World Congress, Vol. 11, pp. 286–290.